Polymer Chemistry

Accepted Manuscript

This is an *Accepted Manuscript*, which has been through the Royal Society of Chemistry peer review process and has been accepted for publication.

Accepted Manuscripts are published online shortly after acceptance, before technical editing, formatting and proof reading. Using this free service, authors can make their results available to the community, in citable form, before we publish the edited article. We will replace this *Accepted Manuscript* with the edited and formatted *Advance Article* as soon as it is available.

You can find more information about *Accepted Manuscripts* in the Information for Authors.

Please note that technical editing may introduce minor changes to the text and/or graphics, which may alter content. The journal's standard Terms & Conditions and the Ethical guidelines still apply. In no event shall the Royal Society of Chemistry be held responsible for any errors or omissions in this *Accepted Manuscript* or any consequences arising from the use of any information it contains.

ROYAL SOCIETY OF CHEMISTRY

www.rsc.org/polymers

Polymer Chemistry

ARTICLE

Synthesis of Highly Refractive and Highly Fluorescent Rigid Cyanuryl Polyimines with Polycyclic Aromatic Hydrocarbon Pendants

Received 00th January 20xx,
Accepted 00th January 20xx

DOI: 10.1039/x0xx00000x

www.rsc.org/

T. Kotaki,[a] N. Nishimura,[b] M. Ozawa,[b] A. Fujimori,[c] H. Muraoka,[a] S. Ogawa,[a] T. Korenaga,[a] E. Suzuki,[a] Y. Oishi,[a] and Y. Shibasaki[a]

A series of rigid cyanuryl polyimines, polyguanamines (PGs) bearing polycyclic aromatic hydrocarbon pendants were successfully synthesized from 2-substituted 4,6-dichloro-1,3,5-triazine and aromatic diamine monomers used in conventional solution polymerization. In addition, their thermal and optical properties were investigated. All polymers showed high thermostabilities (T_g ~ 320°C, T_{d5} (N_2) ~ 466 °C, residue at 800 °C under nitrogen ~ 69.0%) and adequate solubilities in polar organic solvents. Films prepared by the solvent-cast method showed good transparencies, which mainly depended on the diamine structure as opposed to the dichloride moiety. The refractive indices at the D-line (589 nm) of the PG films were unexpectedly high, between 1.677 and 1.800, compared to those of common organic optical polymeric resins. The incorporated melamine moieties afforded effective, dense packing, with the polycyclic aromatic hydrocarbon groups filling the free spaces between rigid polymer chains, resulting in unusually high refractive indices. The PG polymer solution in *N*-methylpyrrolidone showed strong blue fluorescence (371–471 nm) with a quantum yield of up to 98%.

Introduction

Polyguanamines (PGs) are a family of polyimines easily accessible through conventional solution polycondensation, and can be readily modified using 2-substituted 4,6-dichloro-1,3,5-triazine (DCT) as the monomer.[1-9] PG polymers have melamine units that can act as both hydrogen bond donors and acceptors, resulting in the formation of various types of useful supramolecules.[10-16] We previously reported the chemoselective polycondensation of 2-amino-4,6-dichlorotriazine (ADCT) with 4,4'-(9-fluorenylidene)dianiline (BAFL), where the amino functional group on the ADCT monomer was nearly inert during polymerization, resulting in the chemoselective manner.[17] However, BAFL was only the effective diamine monomer to afford high molecular weight soluble polymer (number average molecular weight: M_n = 19,000). We speculated the existence of a multiple-hydrogen interaction between polymeric chains. Taking into account decreasing the melamine-melamine interaction in polymeric materials, we then investigated the polycondensation of 2-*N,N*-dibutylamino-4,6-dichlorotriazine (BDCT) with various aromatic diamines. As expected, the resulting PGs show much better solubility with diamine monomers such as 4,4'-oxydianiline (ODA), *m*-phenylene diamine (*m*PDA).[18] However, it is notable that despite of the introduction of the bulky and flexible *N,N*-dibutyl alkyl substituent, the PG polymers obtained through polycondensation of BDCT with *p*PDA or *o*-tolidine (*o*TD) showed poor solubility in any organic solvents. The measurement of wide angle X-ray diffraction (WAXD) of these bulk PG samples clarified that they were highly crystalline polymers with monoclinic packings. These polymers formed well-aligned nano-spheres or nano-sheets by changing the integration conditions in Langmuir–Blodgett method.[19] These results clearly suggest that the melamine units in the rigid PG main chains have the potential to participate in unique interactions; thus, we expected the formation of highly dense polymeric materials at the melamine units, making them potential candidates for the next generation of highly refractive thermostable organic polymeric resins. Polycyclic aromatic hydrocarbons (PAHs), such as naphthalene, pyrene, and anthracene, are known to be useful in molecular electronic materials in organic electro- and photoluminescent devices, as well as in organic field electronic transistors and fluorescent probes.[20-23] Especially, the fluorescence properties of pyrene have been well studied so far. Aggregation including excimer and exciplex of such chromophores is fatal issue, and

[a] *Department of Chemistry & Bioengineering, Faculty of Engineering, Iwate University, 4-3-5 Ueda, Morioka, Iwate 020-8551, Japan*
[b] *Materials Research Department, Chemical Research Laboratories, Nissan Chemical Industries Ltd., 488-6, Ssuzumi-Cho, Funabashi-shi, Chiba 274-0052, Japan*
[c] *Graduate School of Science and Engineering, Saitama University, 255 Shimo-okubo, Sakura-ku, Saitama 338-8570, Japan.*
Electronic Supplementary Information (ESI) available: See DOI: 10.1039/x0xx00000x

the excited energy is easily lost by the non-radiative transitions.

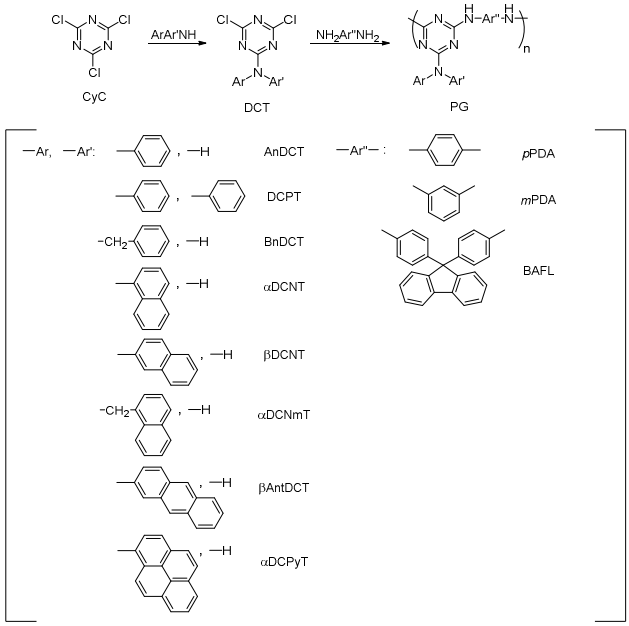

Scheme 1. Synthesis of various polyguanamines (PG)s from CyC.

Thus, encapsulation of chromophores with rigid surroundings such as cyclodextrins[24] and dendrimers[25-27] are of great interest to enhance the fluorescence quantum yield, or to investigate the molecular-level energy transfer phenomena. In this report, we describe the synthesis and properties of aromatic PGs from DCT monomers possessing various PAH structures with amine monomers. The preparation of dense PG structures bearing PAH pendants could be of great interest as well because it can improve understanding of the fluorescence properties of highly dense PG backbones.

Results and discussion

In order to prepare the PG polymers, we first synthesized DCT monomers [2-anilino-4,6-dichloro-1,3,5-triazine (AnDCT), 2,4-dichloro-6-(*N*,*N*-diphenylamino)-1,3,5-triazine (DCPT), 2,4-dichloro-6-(1-naphthylamino)-1,3,5-triazine (αDCNT), 2,4-dichloro-6-(2-naphthylamino)-1,3,5-triazine (βDCNT), 2-benzylamino-4,6-dichloro-1,3,5-triazine (BnDCT), 2,4-dichloro-6-(1-naphthylmethylamino)-1,3,5-triazine (αDCNmT), 2-(2-anthrylamino)-4,6-dichloro-1,3,5-triazine (βAntDCT), and 2,4-dichloro-6-(1-pyrenylamino)-1,3,5-triazine (αDCPyT)] from cyanuric chloride (CyC) with the corresponding amines in THF in the presence of potassium carbonate as a HCl scavenger (Scheme 1). The structures of all of the DCT monomers were identified using IR and NMR spectroscopy, revealing that they had purities adequate for the subsequent polymerization reaction. A series of PG polymers were prepared through conventional solution polycondensation in NMP at 100–200 °C for 6 h in the presence of CsF as a HCl scavenger. To understand the effect of the PAH pendant groups, AnDCT, BnDCT, and DCPT were also prepared and polymerized with diamine monomers, *p*PDA, *m*PDA, and BAFL. BAFL is a well-known diamine monomer, which effectively increase the solubility of the polymeric materials due to the presence of a quaternary carbon atom.[28,29,30,31] In our previous work, ADCT with BAFL was only the case to afford high molecular weight soluble polymer.[17] Figure 1 shows the ^{1}H and ^{13}C NMR spectra of poly(αDCNT-*p*PDA) in DMSO-d_6 at 20 °C. All of the signals were able to be assigned to the expected PG polymer structure. The guanamine hydrogens (NH) in the polymer main chain appeared at 8.95 ppm, which is a upfield shift from 9.11 ppm in the poly(αDCNT-BAFL) sample.

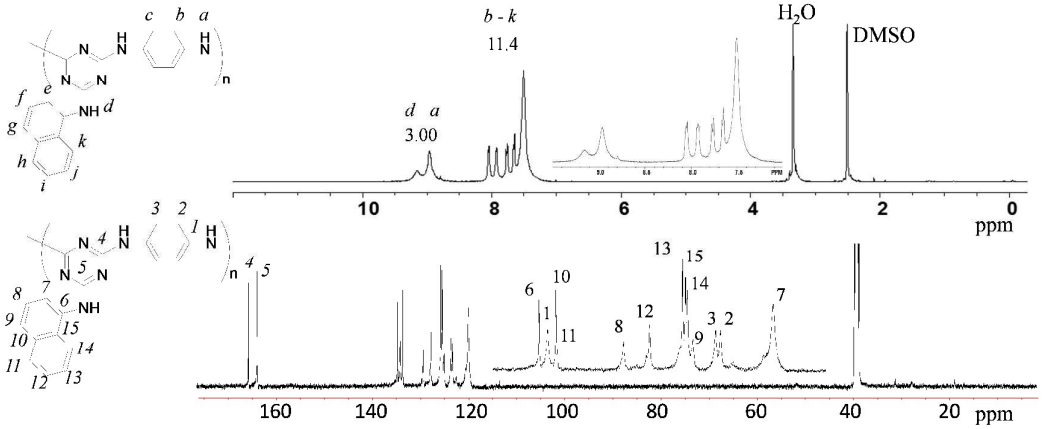

Figure 1. ^{1}H NMR and ^{13}C NMR spectra (DMSO-d_6) of poly(αDCNT-*p*PDA) (run 10, Table 1).

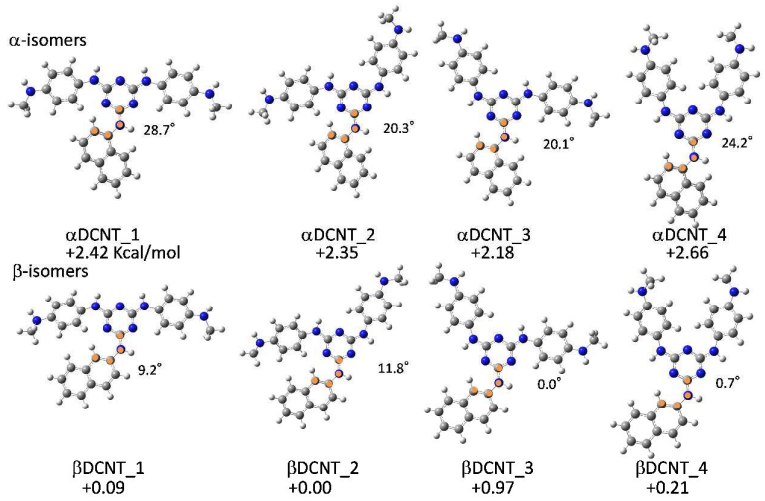

Figure 2. Optimized geometries (B3LYP/6-31G(d) and the dihedral angles of the two model DCNT monomers with the relative energies (kcal/mol).

TABLE 1. Polymerization of DCT with various diamines[a]

Run	DCT			Diamine	Temp (°C)	Yield (%)	M_n[b]	M_w/M_n[b]	n[c]
	Name	R_1	R_2						
1	AnDCT	Ph	H	*p*PDA	110	84[d]	5,100	2.8	18.5
2	AnDCT	Ph	H	*m*PDA	110	82[d]	3,100	2.0	11.2
3	AnDCT	Ph	H	BAFL	100	85[e]	36,100	2.4	69.9
4	DCPT	Ph	Ph	*p*PDA	110	94[d]	1,800	8.3	5.1
5	DCPT	Ph	Ph	*m*PDA	110	94[d]	-	-	-
6	DCPT	Ph	Ph	BAFL	100	92[e]	8,300	2.6	13.3
7	BnDCT	$PhCH_2$	H	*p*PDA	180	75[d]	6,400	5.5	20.0
8	BnDCT	$PhCH_2$	H	*m*PDA	180	81[d]	6,200	2.0	19.4
9	BnDCT	$PhCH_2$	H	BAFL	200	64[e]	10,200	7.9	19.2
10	αDCNT	αNaph	H	*p*PDA	100	90[d]	7,600	14	23.3
11	αDCNT	αNaph	H	*m*PDA	200	77[d]	6,300	3.3	19.3
12	αDCNT	αNaph	H	BAFL	170	76[e]	59,200	4.1	104.5
13	βDCNT	βNaph	H	*p*PDA	100	78[d]	2,000	2.0	6.1
14	βDCNT	βNaph	H	*m*PDA	200	85[d]	3,900	4.8	11.9
15	βDCNT	βNaph	H	BAFL	170	93[e]	12,000	4.0	21.2
16	αDCNmT	α$NaphCH_2$	H	*p*PDA	180	92[d]	6,700	4.5	19.7
17	αDCNmT	α$NaphCH_2$	H	*m*PDA	180	91[d]	4,300	2.3	12.6
18	αDCNmT	α$NaphCH_2$	H	BAFL	200	63[e]	9,600	10.2	15.7
19	βAntDCT	βAnthryl	H	*p*PDA	100	90[d]	3,200	2.0	8.5
20	βAntDCT	βAnthryl	H	*m*PDA	200	90[d]	2,700	1.6	7.2
21	βAntDCT	βAnthryl	H	BAFL	180	95[e]	17,000	7.4	27.5
22	αDCPyT	αPyrenyl	H	*p*PDA	100	94[d]	2,700	2.3	6.5
23	αDCPyT	αPyrenyl	H	*m*PDA	200	95[d]	6,500	2.1	15.7
24	αDCPyT	αPyrenyl	H	BAFL	180	75[e]	9,000	11.1	13.9

[a] Conditions; Monomers = 1.0 mmol, CsF = 2.2 mmol, NMP =2 mL, 6 h. [b] Determined by GPC (NMP with LiBr, PSt) . [c] Repeating number of polymer structure. [d] Purified only by washing with hot MeOH. [e] Purified by reprecipitation with MeOH.

For the poly(βDCNT-*p*PDA) and poly(βDCNT-BAFL) polymers, these signals appeared at 9.44 ppm and 9.40 ppm, respectively. Due to the steric hindrance between the naphthalene and triazine rings, the α-naphthyl isomer should possess a twisted structure between these two rings, decreasing the resonance effect and increasing the electron density of the triazine ring. The optimized geometry calculated by the density functional theory method (B3LYP/6-31G(d)) also supported this assumption. The model compound containing the α–isomer has four optimized geometries, whose energy ranges are within 0.44 kcal/mol. The dihedral angles of the C(sp^2)–N and naphthalene rings for these conformers range from 20.1° to 28.7° (Figure 2). The model compound containing the β-isomer also has four stable geometries, whose energy ranges are within 0.97 kcal/mol. It is noteworthy that the dihedral angles of these isomers range from 0° to

11.8°, which are much smaller than those of the α-isomers. The inductive effect of the PAH pendants can be observed in the NMR spectra; poly(AnDCT-BAFL) main-chain NH at 9.23 ppm, poly(DCPT-BAFL) main-chain NH at 9.15 ppm, poly(DCPyT-BAFL) main-chain NH at 9.64 ppm, and poly(AntDCT-BAFL) main-chain NH at 9.50 ppm. That is, the coplanar PAH pendants expanded the resonance in the polymer skeleton.

The polymerization results are summarized in Table 1. The polymerization of AnDCT with BAFL in NMP afforded the PG [poly(AnDCT-BAFL)] with a high M_n of 36,100 and a reasonable M_w/M_n value of 2.4 in an 85% yield (run 3). Conversely, only low- M_n PGs were obtained from AnDCT with *p*PDA or *m*PDA, mainly due to the poor solubility of the resulting polymers. PGs consisting of *m*PDA potentially possess structures more bent than those of PGs consisting of *p*PDA; thus, they should have better solubilities and afford higher- M_n polymers. However, the M_n values of the resulting PGs bearing *m*PDA units were lower than the values of those with *p*PDA, most likely due to the formation of cyclic oligomers. The bimodal peak in GPC traces for PGs bearing *m*PDA units supported this assumption. The BnDCT monomer required a higher polymerization temperature due to the electron-donating effect of the substituent, which was expected decrease the polymerizabilities of the dichloride monomers (runs 7, 8, and 9). For the polymerization of DCPT with diamines, only low- M_n polymers were obtained (runs 4 and 6).

TABLE 2. Solubility of PGs [a]

Polymer	DMF	DMAc	NMP	DMSO	THF	GBL	PGMEA	CHN
Poly(AnDCT-*p*PDA)	±	±	++	++	−	±	−	−
Poly(AnDCT-*m*PDA)	++	++	++	++	++	++	−	+
Poly(AnDCT-BAFL)	++	++	++	++	++	++	−	+
Poly(DCPT-*p*PDA)	++	±	+	−	−	±	−	−
Poly(DCPT-*m*PDA)	−	−	−	−	−	−	−	−
Poly(DCPT-BAFL)	++	++	++	++	++	++	−	++
Poly(αDCNT-*p*PDA)	±	±	++	++	−	−	−	−
Poly(αDCNT-*m*PDA)	++	++	++	++	−	++	−	+
Poly(αDCNT-BAFL)	++	++	++	++	++	++	−	±
Poly(BnDCT-*p*PDA)	±	±	±	+	−	−	−	−
Poly(BnDCT-*m*PDA)	+	++	++	++	++	+	−	−
Poly(BnDCT-BAFL)	++	++	++	++	++	+	−	−
Poly(αDCNmT-*p*PDA)	−	−	+	+	−	−	−	−
Poly(αDCNmT-*m*PDA)	++	±	±	±	+	+	−	−
Poly(αDCNmT-BAFL)	++	++	++	++	++	±	−	±
Poly(βDCNT-*p*PDA)	++	++	++	++	±	−	−	±
Poly(βDCNT-*m*PDA)	++	++	++	++	++	++	−	++
Poly(βDCNT-BAFL)	++	++	++	++	++	++	−	++
Poly(βAntDCT-*p*PDA)	++	++	++	++	−	−	−	±
Poly(βAntDCT-*m*PDA)	++	++	++	++	+	++	−	++
Poly(βAntDCT-BAFL)	++	++	++	++	±	++	−	++
Poly(αDCPyT-*p*PDA)	±	±	±	±	−	−	−	±
Poly(αDCPyT-*m*PDA)	++	++	++	++	++	±	−	++
Poly(αDCPyT-BAFL)	++	++	++	±	−	−	−	±

[a] Polymer 10 mg / Solvent 5 mL (++ soluble at room temperature; + soluble after heating; ± partially insoluble; - insoluble). DMF; *N*,*N*-dimethylformamide, DMAc; *N*,*N*-dimethylacetamide, NMP; *N*-methyl-2-pyrrolidone, DMSO; dimethyl sulfoxide, THF; tetrahydrofuran, GBL; γ-butyrolactone, PGMEA; propylene glycol monomethyl ether acetate, CHN; cyclohexanone.

Especially, the PG polymer from *p*PDA with DCPT showed bimodal profile in GPC, indicating the favourable formation of cyclic oligomers (Figure S35). In the case of DCT monomers having PAH pendants, PGs with high M_n values were successfully obtained (runs 10–24). αDCNT yielded high-M_n PG polymers more effectively than the β-isomer did. Table 2 shows the results of the polymer solubility test in various organic solvents. All as-prepared polymers initially showed excellent solubilities; however, after drying at 200 °C under a vacuum to remove the residual solvents, their solubilities worsened significantly. We currently speculate that PGs might form multiple hydrogen bonding networks between polymer chains at the melamine units upon removal of the solvent, as described below. As a diamine monomer, BAFL is quite effective at yielding sufficiently soluble PG samples. The poly(αDCNT-BAFL) sample gave the highest M_n value of 59,200, due to the twisted structure of the triazine-α-naphthyl moiety, which makes the polymer sufficiently soluble during the polymerization. However, despite of the high solubility and very high M_n, the poly(αDCNT-BAFL) polymer film casted from NMP was brittle, and thus we were not able to evaluate the mechanical properties of it.

TABLE 3. Thermal properties of PGs [a]

Polymer	M_n [a]	T_g [b]	TGA (N_2) T_{d5} [c]	TGA (N_2) T_{d10} [c]	TGA (N_2) Residue at 800°C
Poly(AnDCT-*p*PDA)	5,100	225	352	405	52.6
Poly(AnDCT-*m*PDA)	3,100	209	418	445	58.0
Poly(AnDCT-BAFL)	36,100	287	448	468	54.5
Poly(DCPT-*p*PDA)	1,800	-	417 [d]	465 [d]	35.9 [d]
Poly(DCPT-*m*PDA)	-	-	439	470	35.1
Poly(DCPT-BAFL)	8,300	-	466	483	47.8
Poly(αDCNT-*p*PDA)	7,600	234	439	453	53.5
Poly(αDCNT-*m*PDA)	6,300	218	440	462	67.2
Poly(αDCNT-BAFL)	59,200	288	447	467	56.0
Poly(BnDCT-*p*PDA)	6,400	204	440	453	59.3
Poly(BnDCT-*m*PDA)	6,200	187	414	434	58.3
Poly(BnDCT-BAFL)	10,200	266	453	468	60.9
Poly(αDCNmT-*p*PDA)	6,700	206	442	452	58.4
Poly(αDCNmT-*m*PDA)	4,300	191	413	431	57.6
Poly(αDCNmT-BAFL)	9,600	265	453	465	60.3
Poly(βDCNT-*p*PDA)	2,000	226	430	451	60.6
Poly(βDCNT-*m*PDA)	3,900	225	427	449	60.3
Poly(βDCNT-BAFL)	12,000	297	445	463	58.0
Poly(βAntDCT-*p*PDA)	3,200	240	441	461	63.8
Poly(βAntDCT-*m*PDA)	2,700	235	449	467	68.6
Poly(βAntDCT-BAFL)	17,000	305	455	472	58.9
Poly(αDCPyT-*p*PDA)	2,700	274	420	452	55.4
Poly(αDCPyT-*m*PDA)	6,500	261	444	464	69.0
Poly(αDCPyT-BAFL)	34,800	320	457	484	62.9

[a] Determined by GPC (NMP with 0.01 wt% of LiBr). [b] Determined by DSC in nitrogen at a heating rate of 20 °C/min. [c] T_{d5} and T_{d10} are the temperatures for 5 % and 10 % decomposition of the polymers, respectively (in nitrogen, heating rate 10 °C/min). [d] Two-stage weight loss was observed.

The solubility test was performed using different M_n samples; thus, we assumed that the poly(αDCNT-BAFL) sample would be more soluble than the β-isomer with the same M_n. Compared to anilino and *N*,*N*-diphenylamino groups, PAH

pendants, including naphthyl and pyrenyl groups, effectively suppressed the polymer main chain packing, resulting in high M_n polymers.

Table 3 shows the thermal properties of the PG samples. The glass transition temperatures (T_g) of the polymers range from 187 °C to 320 °C, with the polymers containing BAFL units possessing T_g values higher than those of the other PG samples.

This phenomenon is well known and can be explained by the effect of the bulky pendant fluorenyl moiety, which restricts the rotation of the polymer main chains.

TABLE 4. Refractive indices and Abbe's numbers of PG films [a]

Polymer	Thickness (nm)	n_F [b]	n_D [b]	n_C [b]	ν [c]
Poly(AnDCT-*m*PDA)	128	1.824	1.783	1.769	14
Poly(AnDCT-BAFL)	288	1.734	1.709	1.703	23
Poly(DCPT-BAFL)	154	1.760	1.728	1.715	16
Poly(αDCNT-*p*PDA)	166	1.852	1.800	1.783	12
Poly(αDCNT-BAFL)	277	1.781	1.745	1.734	16
Poly(αDCNmT-BAFL)	299	1.752	1.722	1.711	18
Poly(αDCPyT-BAFL)	322	1.845	1.786	1.770	11

[a)] Film thickness: 128 - 322 nm. [b)] Refractive index at F-line (481 nm), D-line (589 nm), C-line (656 nm). [c)] Abbe's number.

In our previous work, the T_g values of poly(ADCT-BAFL) and poly(BDCT-BAFL) were determined to be 266 °C and 237 °C, respectively,[17,18] suggesting that the introduction of a PAH unit more effectively suppresses the chain movement in the polymeric structure than an amino group (NH_2) does on the ADCT unit. The high thermostability was confirmed by the 5 wt%-loss temperature (T_{d5}) above 352 °C, which is attributable to completely aromatic polymeric structures. This unusual data was found in the residues at 800 °C under a nitrogen stream. With the exception of PGs from the DCPT monomer, the char yields of the polymers ranged from 58% to 69%. Their excellent high-flame retardancies could be explained by the existence of the triazine group in conjunction with the PAH moieties, which can form N-rich thin skin layers on the surfaces of the materials.[32]

Table 4 shows the refractive indices and Abbe numbers measured using the ellipsometry technique. The film thickness was adjusted to approximately 200 nm using the 5 wt% polymer solution in NMP/cyclohexanone (9:1 v/v), in which almost all PG samples dried at 200 °C in N_2 were not homogeneously soluble, as described above. Thus, for the refractive index measurement, the polymer samples dried at 20 °C were used. Nonetheless, the maximum refractive index at the D-line (587.6 nm) is 1.800, which is extraordinarily high compared to the refractive indices of conventional optical organic resins such as polycarbonate (PC) (n_{633nm} = 1.590), Kapton® (n_{633nm} = 1.695), *S*-polyimide (30% *S* content, n_{633nm} = 1.768), PC from 9,9-bis(4-hydroxyphenyl)fluorene monomer (n_{587nm} = 1.661), and triazine-containing poly(phenylene thioether) (n_{587nm} = 1.749).[33,34,35]

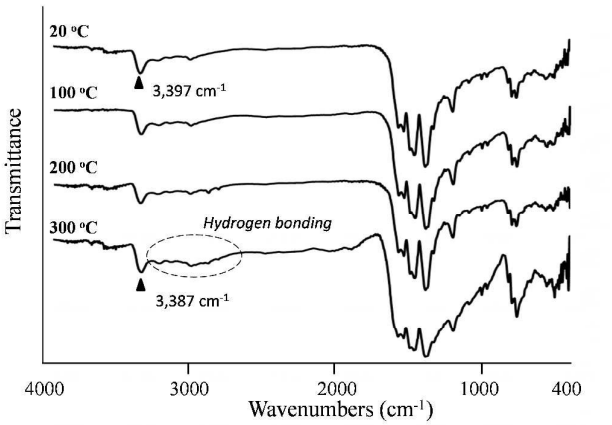

Figure 3. IR spectra of poly(aDCNT-*p*PDA) film heated at 20, 100, 200, and 300 ° C for 2 h each.

The high refractive indices can be attributed to the high contents of melamine units with wholly aromatic structure, which can effectively pack polymers including multiple hydrogen bonding networks, and PAH pendants, which can effectively fill spaces between polymer backbones.

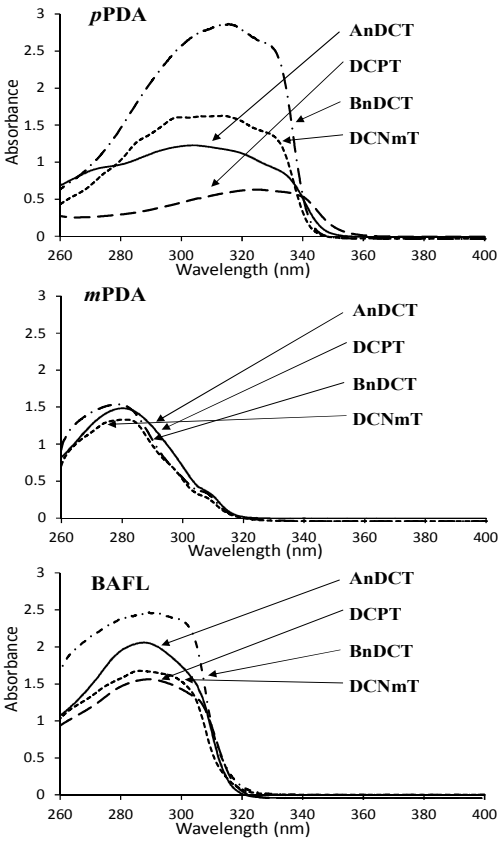

Figure 4. UV-vis spectra of polymers in NMP (7.5×10^{-2} mmol/L).

In order to confirm the existence of multiple hydrogen bonding networks between PG samples, change in the IR spectra was carefully monitored upon heating of the polymer samples (Figure 3). Poly(αDCNT-*p*PDA) samples were freshly prepared and dried at 20 °C, 100 °C, 150 °C, 200 °C, and 300 °C under air for 2 h each. As shown, the sharp absorption peak observed at 3,397 cm^{-1} for the N–H stretching of the parent PG sample [poly(αDCNT-*p*PDA)] dried at 20 °C shifts to a lower wavenumber of 3,387 cm^{-1}, with the broad absorptions around 3,000 cm^{-1} increasing with drying temperature up to 300 °C. The polymer sample cured at 300 °C became almost insoluble in NMP/cyclohexanone (9:1 v/v), refractive index solvent, though the other IR absorption peaks did not change significantly. This can be observed for the other PG samples as well.

To investigate the local packing within the polymeric structures in detail, we performed UV-vis and fluorescence studies. Figure 4 depicts the UV-vis spectra of PG polymers consisting of AnDCT, DCPT, BnDCT, or αDCNmT with diamine monomers of *p*PDA, *m*PDA, or BAFL. As can be seen from these spectra, the λmax and absorption edge were strongly affected by the diamine structure, not the DCT monomer. However, for the series of PAH pendant PG samples, poly(αDCPyT-BAFL) and poly(βAntDCT- BAFL), the spectra were also affected by the pendant group (Figure 5). For the PG samples consisting of the βAntDCT monomer, *p*PDA, *m*PDA, and BAFL do not seem to affect the absorption spectra significantly, and they have vibrational structures that are clearer than and slightly different from those of monomeric βAntDCT. Similarly, for the PG samples consisting of the αDCPyT monomer, the diamine monomer structures do not seem to affect the absorption spectra significantly, and they have vibrational structures that are clearer than and slightly different from those of monomeric αDCPyT. These differences could be attributable to the cage effect within the rigid PG structures.

Figure 6 depicts the fluorescence spectra of the DCT monomers and PG samples in NMP. The fluorescence data are summarized in Table 5. For αDCNT samples, the monomer solution exhibits λ_{em} at 385.7 nm with a Φ_{fl} of 1.4%, whereas the poly(αDCNT-*p*PDA) sample shows a large hypsochromic shift (λ_{em} at 471.8 nm), while maintaining a similar Φ_{fl} value. In contrast, the PG samples consisting of *m*PDA and BAFL show small bathochromic shifts with larger Φ_{fl} values of 24% and 27%. For the βDCNT samples, the monomer solution has λem at 378.1 nm with a Φ_{fl} of 8.2%, whereas the poly(βDCNT-*p*PDA) sample also shows a large hypsochromic shift (λ_{em} at 439.4 nm), resulting in a slightly smaller Φ_{fl} value of 3.4%. In contrast, the PG samples consisting of *m*PDA and BAFL show small bathochromic shifts with larger Φ_{fl} values of 37% and 70%. For the βAntDCT samples, the results are similar; however, the λ_{em} of the poly(βAntDCT-*p*PDA) sample solution is nearly identical to that of the monomer. It can be seen that the poly(βAntDCT-BAFL) solution shows almost quantitative fluorescence (Φ_{fl} = 98%).

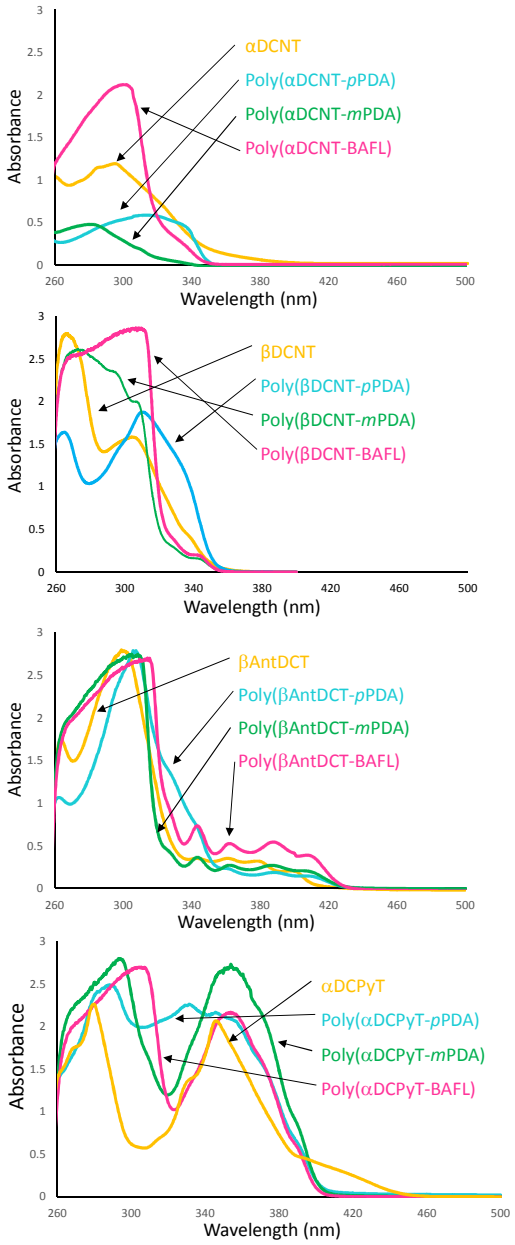

Figure 5. UV-vis spectra of monomers and polymers in NMP (7.5×10^{-2} mmol/L).

Finally, for the αDCPyT samples, all of the PG polymers show bathochromic shifts with higher Φ_{fl} values. The PAH groups in the αDCNT and αDCPyT samples are connected at the α-positions with the triazine ring; thus, the two rings are twisted. As such, the Φ_{fl} values are much lower than the PG samples containing βDCNT and βAntDCT. The higher Φ_{fl} values for the PG samples compared to those of the original monomers can be explained by the effective isolation and confinement of the

PAH groups within the rigid rods and the bulky polymeric skeletons.

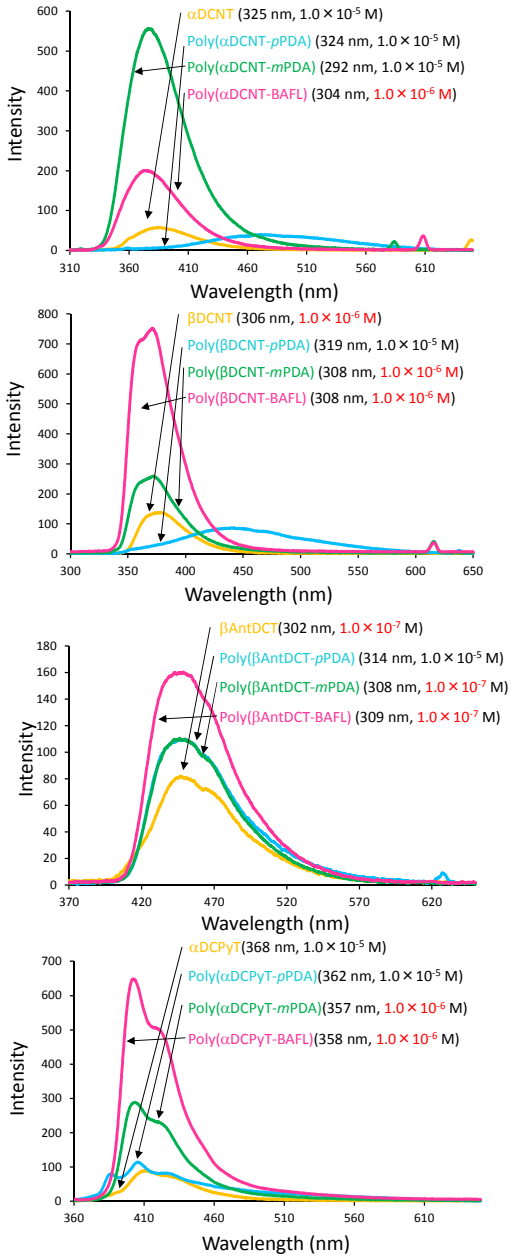

Figure 6. Fluorescence spectra of monomers and polymers in NMP.

To determine why the Φ_{fl} values of the PG solution bearing PDA segments are extremely low, and the large hypsochromic effects in the fluorescence spectra are observed, the effect of the poly(βDCNT-*m*PDA) sample concentration on the fluorescence spectra was investigated (Figure 7). As the concentration of the polymer solution increases from 1.0×10^{-6} M to 1.0×10^{-2} M, the fluorescence intensity at 372.4 nm dramatically decreases and weak, broad fluorescence are observed at 450 nm and 616 nm, which could be due to the excimer or exciplex formation of the chromophore in the polymeric chain. However, taking account the absence of the UV absorption below 350 nm in the excitation spectrum (Figure 7C), and the vibrations only observed at 450 nm emission (not at 616.2 nm emission) in the fluorescence spectrum (Figure 7D), the reason of the low Φ_{fl} values and the large hypsochromic effects could be mainly attributable to the formation of aggregated species in concentrated medium.

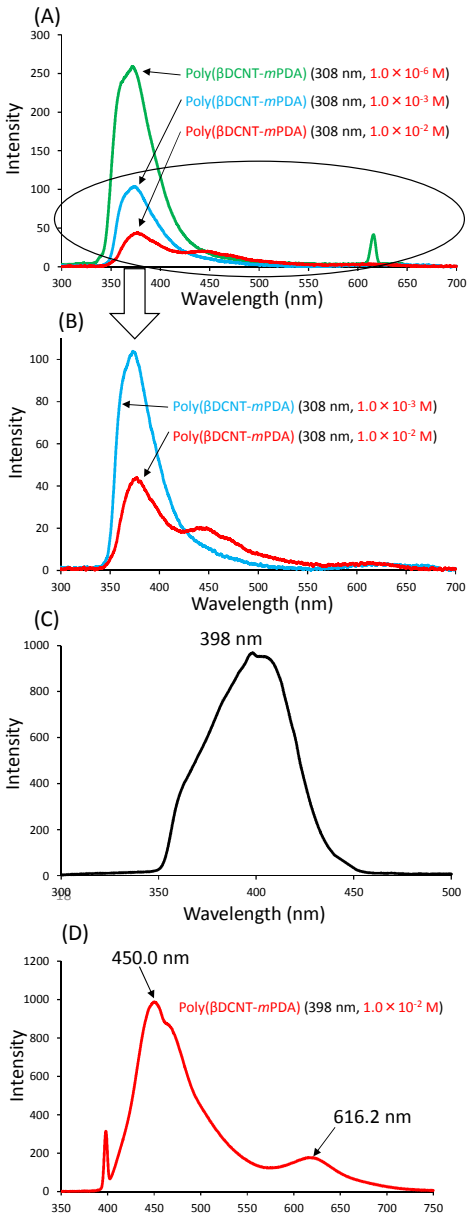

Figure 7. The fluorescence spectra of poly(βDCNT-mPDA) in NMP at various concentrations (A), (B). The excitation spectrum for the 450.0 nm emission (C). The fluorescence spectrum excited at 398 nm (D).

TABLE 5. Excitation and emission wavelength of PG solutions, and the quantum efficiencies

Compound	λ_{ex} [a] (nm)	λ_{em} [b] (nm)	Φ_{fl} [c] (%)
αDCNT	324.5	385.7	1.4
Poly(αDCNT-*p*PDA)	324.4	471.8	1.9
Poly(αDCNT-*m*PDA)	292.1	376.7	24
Poly(αDCNT-BAFL)	304.4	374.3	26.5
βDCNT	305.6	378.1	8.2
Poly(βDCNT-*p*PDA)	319.2	439.4	3.4
Poly(βDCNT-*m*PDA)	308.1	372.4	37
Poly(βDCNT-BAFL)	308.2	371.0	70
βAntDCT	302.3	446.6	75
Poly(βAntDCT-*p*PDA)	314.2	447.8	2.2
Poly(βAntDCT-*m*PDA)	307.9	446.1	78
Poly(βAntDCT-BAFL)	308.7	442.3	98
αDCPyT	367.5	411.2	0.6
Poly(αDCPyT-*p*PDA)	362.0	405.5	0.9
Poly(αDCPyT-*m*PDA)	357.4	403.9	14
Poly(αDCPyT-BAFL)	357.6	402.5	27

[a] The excitation wavelength. [b] The maximum emission wavelength. [c] Quantum yield of the emission.

Experimental

Materials. Dioxane, tetrahydrofuran (THF), and *N*-methylpyrrolidone (NMP) were dried over calcium hydride (CaH_2) and distilled under reduced pressure prior to use. Cesium fluoride (CsF) was dried at 180 °C for 12 h under reduced pressure before use. *m*PDA and *p*PDA were used after sublimation. BAFL was purified through recrystallization from ethanol before use. β-Naphthylamine was prepared according to a literature procedure.[36] All other reagents and solvents were used as received.

Synthesis of 2-anilino-4,6-dichloro-1,3,5-triazine (AnDCT). This monomer was prepared according to a modified literature procedure.[37] In a three-neck flask equipped with an addition funnel and a magnetic stirrer, CyC (55.46 g, 0.300 mol) was dissolved in THF (150 mL) and cooled to 0 °C. To this solution, aniline (28.26 g, 0.300 mmol) and THF (80 mL) were added dropwise. After stirring for 2 h, a solution of Na_2CO_3 (19.96 g, 0.190 mol) in distilled water (100 mL) was added dropwise at 0 °C. After stirring for an additional 2 h, the reaction solution was transferred to a separatory funnel and washed three times with brine. The organic layer was dried over $MgSO_4$ and filtered. The filtrate was concentrated under reduced pressure to produce a white solid. The product was purified by recrystallization from toluene/n-hexane and sublimated (120 °C, 0.03 mmHg). Yield 43.4 g (60.0%). mp 133–134 °C (lit136–138 °C). ^{1}H NMR (400 MHz, DMSO-d_6, ppm) δ 7.19 (t, 1H, p-Ar-H), 7.40 (dd, 2H, m-Ar-H), 7.60 (d, 2H, o-Ar-H), 11.16 (s, 1H, N–H). ^{13}C NMR (100 MHz, DMSO-d_6, ppm) δ 121.9, 125.4, 129.3, 137.4, 164.2, 169.3, 170.2.

Synthesis of 2,4-dichloro-6-(*N*,*N*-diphenylamino)-1,3,5-triazine (DCPT). This monomer was prepared according to a modified literature procedure.[38] The detailed procedure was similar to that used to synthesize AnDCT, with the exception of triethylamine being used in place of aqueous Na_2CO_3. The product was purified by recrystallization from toluene/hexanes and sublimated (140 °C, 0.03 mmHg). This process afforded a white powder in a 47.0% yield. mp 175.0–176.5 °C (lit172–173 °C). ^{1}H NMR (400 MHz, $CDCl_3$, ppm) δ 7.26 (d, 4H, o-Ar-H), 7.28 (t, 2H, p-Ar-H), 7.41 (t, 4H, m-Ar-H). ^{13}C NMR (100 MHz, $CDCl_3$, ppm) δ 127.0, 127.4, 129.3, 141.4, 165.7, 170.4.

2,4-Dichloro-6-(1-naphthylamino)-1,3,5-triazine (αDCNT). This monomer was prepared according to a modified literature procedure.[39] The product was purified by recrystallization from toluene/hexanes and sublimated (165 °C, 0.03 mmHg). This process afforded a white powder in a 70% yield. mp 162.0–163.0 °C (lit142 °C). FT-IR [KBr (cm^{-1})]: 3381, 3225 (N–H), 3080 (C–H), 1596 (N–H bending), 1542 (C=C), 1508 (C=N), 1229 (C–N), 845 (C–Cl). ^{1}H NMR (400 MHz, DMSO-d_6, ppm) δ 7.57–7.58 (m, 4H, Ar-H), 7.93–7.99 (m, 3H, Ar-H), 11.2 (s, 1H, N–H). ^{13}C NMR (100 MHz, DMSO-d_6, ppm) δ 123.3, 124.5, 126.1, 126.9, 127.0, 127.9, 128.7, 129.3, 132.4, 134.3, 166.4, 169.6, 170.2. Elemental analysis (C13H8Cl2N4) calcd (%) C: 53.63, H: 2.77, N: 19.24; found (%) C: 53.71, H: 2.69, N: 19.27.

2,4-Dichloro-6-(2-naphthylamino)-1,3,5-triazine (βDCNT). This compound was prepared by a method similar to that used to produce AnDCT. The product was purified by recrystallization from 1,4-dioxane/hexanes and sublimated (165 °C, 0.06 mmHg). This process afforded a white powder in a 68% yield. mp 160.0–161.0 °C. FT-IR [KBr (cm^{-1})]: 3284 (N–H), 3083 (C–H), 1616, 1596 (N–H bending), 1556 (C=C), 1511 (C=N), 1220 (C–N), 855 (C–Cl). ^{1}H NMR (400 MHz, DMSO-d_6, ppm) δ 7.46–7.54 (m, 2H, Ar-H), 7.70–7.73 (d, 1H, Ar-H), 7.85–7.96 (m, 3H, Ar-H), 8.14 (s, 1H, Ar-H), 11.36 (s, 1H, N–H). ^{13}C NMR (100 MHz, DMSO-d_6, ppm) δ 118.7, 121.7, 125.9, 127.1, 127.8, 127.9, 128.9, 130.8, 133.3, 134.9, 164.2, 169.1, 170.1. Elemental analysis (C13H8Cl2N4) calcd (%) C: 53.63, H: 2.77, N: 19.24; found (%) C: 53.59, H: 2.87, N: 19.33.

2-Benzylamino-4,6-dichloro-1,3,5-triazine (αBnDCT). This monomer was prepared according to a modified literature procedure.[40] The product was purified by recrystallization from tetrahydrofuran/hexanes and sublimated (130 °C, 0.06 mmHg). This process afforded a white powder in a 59% yield. mp 115–117 °C (lit120–122 °C). FT-IR [KBr (cm^{-1})]: 3259 (N–H), 3175, 3112 (C–H), 1626 (N–H bending), 1550 (C=C), 1516 (C=N), 1238 (C–N), 849 (C–Cl). ^{1}H NMR (400 MHz, DMSO-d_6, ppm) δ 4.53 (d, 2H, -CH2), 7.25–7.35 (m, 5H, Ar-H), 9.12 (t, 1H, -NH). ^{13}C NMR (100 MHz, DMSO-d_6, ppm) δ 44.0, 127.2, 127.3, 128.5, 137.5, 165.5, 168.7, 169.6. Elemental analysis (C10H8Cl2N4) calcd (%) C: 47.08, H: 3.16, N: 21.96; found (%) C: 47.03, H: 3.22, N: 22.14.

2,4-Dichloro-6-(1-naphthylmethylamino)-1,3,5-triazine (αDCNmT). This compound was prepared by a method similar to that used to produce AnDCT. The product was purified by recrystallization from tetrahydrofuran/hexanes and sublimated (180 °C, 0.06 mmHg). This process afforded a white powder in a 70% yield. mp 190–192 °C. FT-IR [KBr (cm^{-1})]: 3242 (N–H), 2879 (C–H), 1604 (N–H bending), 1545 (C=C), 1508 (C=N), 1238 (C–N), 844 (C–Cl). ^{1}H NMR (400 MHz, DMSO-d_6,

ppm) δ 4.98 (d, 2H, -CH2), 7.48 (m, 2H, Ar-H), 7.57 (m, 2H, Ar-H), 7.88 (d, 1H, Ar-H), 7.97 (d, 1H, Ar-H), 8.10 (d, 1H, Ar-H), 9.71 (t, 1H, -NH). ^{13}C NMR (100 MHz, DMSO-d_6, ppm) δ 42.3, 123.3, 125.4, 129.5, 126.0, 126.5, 128.0, 128.6, 130.7, 132.5, 133.3, 165.5, 168.7, 169.6. Elemental analysis (C14H10Cl2N4) calcd (%) C: 55.10, H: 3.30, N: 18.36; found (%) C: 55.11, H: 3.38, N: 18.51.

2-(2-Anthrylamino)-4,6-dichloro-1,3,5-triazine (βAntDCT). This monomer was prepared according to a modified literature procedure.[41] The product was purified by recrystallization from toluene/hexanes. This process afforded yellow needle crystals in a 47% yield. mp 216–217 °C (lit.219–221 °C). FT-IR [KBr (cm^{-1})]: 3242 (N–H), 2879 (C–H), 1595 (bending N–H), 1548 (C=C), 1508 (C=N), 1233 (C–N), 835 (C–Cl). ^{1}H NMR (400 MHz, DMSO-d_6, ppm) δ 7.49–7.53 (m, 2H, Ar-H), 7.68 (d, 1H, Ar-H), 8.06–8.12 (m, 3H, Ar-H), 8.35 (s, 1H, Ar-H), 8.54 (d, 2H, Ar-H), 11.4 (s, 1H, N–H). ^{13}C NMR (100 MHz, DMSO-d_6, ppm) δ 117.6, 122.0, 125.6, 125.8, 126.1, 126.3, 128.0, 128.3, 129.1, 129.2, 131.1, 131.2, 132.0, 164.1, 169.0, 170.0. Elemental analysis (C17H10Cl2N4) calcd (%) C: 59.84, H: 2.95, N: 16.42; found (%) C: 59.86, H: 2.99, N: 16.38.

2,4-Dichloro-6-(1-pyrenylamino)-1,3,5-triazine (αDCPyT). This monomer was prepared according to a modified literature procedure.[42] The product was purified by recrystallization from 1,4-dioxane/hexanes. This process afforded a white powder in a 63% yield. mp 228–230 °C (lit.236–237 °C). FT-IR [KBr (cm^{-1})]: 3223 (N–H), 3090 (C–H), 1603 (N–H bending), 1548 (C=C), 1508 (C=N), 1232 (C–N), 848 (C–Cl). ^{1}H NMR (400 MHz, DMSO-d_6, ppm) δ 8.06–8.34 (m, 9H, Ar-H), 11.561 (s, 1H, -NH). ^{13}C NMR (100 MHz, DMSO-d_6, ppm) δ 122.4, 123.7, 124.4, 124.9, 125.1, 125.6, 125.7, 125.8, 126.7, 127.2, 127.6, 128.0, 129.7, 129.8, 130.5, 130.7, 166.0, 169.3, 169.9. Elemental analysis (C19H10Cl2N4) calcd (%) C: 62.48, H: 2.76, N: 15.34; found (%) C: 62.71, H: 2.88, N: 15.29.

Synthesis of PGs from DCT monomers with aromatic diamines. Typical procedure [poly(αDCNT-pPDA)]. All of the glass vessels were heated under a vacuum before use and were filled with and handled in a stream of dry nitrogen. In a two-neck flask equipped with a three-way stopcock, reflux condenser, and magnetic stirrer, *p*PDA (0.108 g, 1.00 mmol) was dissolved in dry NMP (2 mL) at room temperature. To this solution, αDCNT (0.291 g, 1.00 mmol) and CsF (0.334 g, 2.20 mmol) were added sequentially. The mixture was stirred for 10 min, followed by polymerization at 100 °C for 6 h. The polymerization solution was then cooled to room temperature and poured into an excess amount of methanol containing NH_3(aq) in order to remove the HCl and inorganic salts generated from the reaction, as well as to remove excess CsF. The fibrous precipitate was dried at 60 °C for 12 h, washed with hot methanol, and dried at 180 °C for 12 h under reduced pressure. This procedure yielded 0.32 g (90%). FT-IR [KBr (cm^{-1})]: 3398 (guanamine hydrogen), 3050 (aromatic C–H), 1558 (aromatic C=C), 1486 (triazine C=N), 1407, 805 (aromatic C–H), 1216 (aromatic C–N). ^{1}H NMR (400 MHz, DMSO-d_6, ppm) δ 7.50–8.04 (Ar-H), 8.95, 9.15 (-NH-). ^{13}C NMR (100 MHz, DMSO-d_6, ppm) δ 120.2, 123.5, 123.8, 125.3, 125.6, 125.7, 125.9, 128.0, 129.6, 133.8, 133.9, 134.4, 134.9, 164.1, 165.9.

Poly(αDCNT-*m*PDA). FT-IR [KBr (cm^{-1})]: 3399 (N–H), 3280–3100 (amine and guanamine hydrogen bonding), 3052 (aromatic C–H), 1579 (aromatic C=C), 1477 (triazine C=N), 1415, 806 (aromatic C–H), 1194 (aromatic C–N). ^{1}H NMR (400 MHz, DMSO- d_6, ppm) δ 6.67–8.04 (Ar-H), 8.22, 9.24 (-NH-).

Poly(αDCNT-BAFL). FT-IR [KBr (cm^{-1})]: 3396 (N–H), 3330–3100 (amine and guanamine hydrogen bonding), 3052 (aromatic C–H), 1595, 1568 (aromatic C=C), 1480 (triazine C=N), 1412, 807, 747, 733 (aromatic C–H), 1185 (aromatic C–N). ^{1}H NMR (400 MHz, DMSO-d_6, ppm) δ 6.85–7.96 (Ar-H), 9.11 (-NH-).

Poly(βAnDCT-*p*PDA). FT-IR [KBr (cm^{-1})]: 3399 (N–H), 3290–3100 (amine and guanamine hydrogen bonding), 3050–3033 (aromatic C–H), 1576, 1559 (aromatic C=C), 1490 (triazine C=N), 1406, 804, 751, 691 (aromatic C–H), 1213 (aromatic C–N). ^{1}H NMR (400 MHz, DMSO-d_6, ppm) δ 6.91–7.03, 7.04, 7.23, 7.51, 7.78, 7.88, 7.89 (Ar-H), 9.10, 9.18, 9.47 (-NH-).

Poly(βAnDCT-*m*PDA). FT-IR [KBr (cm^{-1})]: 3408 (N–H), 3880–3110 (amine and guanamine hydrogen bonding), 3032–3056 (aromatic C–H), 1577, 1557 (aromatic C=C), 1507 (triazine C=N), 1410, 805, 751, 689 (aromatic C–H), 1226 (aromatic C–N). ^{1}H NMR (400 MHz, DMSO-d_6, ppm) δ 5.76 (terminal NH_2), 6.53–6.54, 6.89, 6.97, 7.07, 7.28, 7.74, 7.83 (Ar-H), 9.16 (-NH-).

Poly(βAnDCT-BAFL). FT-IR [KBr (cm^{-1})]: 3398 (N–H), 3290–3110 (amine and guanamine hydrogen bonding), 3032 (aromatic C–H), 1575 (aromatic C=C), 1505, 1489 (triazine C=N), 1411, 806, 748, 690 (aromatic C–H), 1232 (aromatic C–N). ^{1}H NMR (400 MHz, DMSO-d_6, ppm) δ 6.91–6.93, 7.01, 7.18, 7.26, 7.34, 7.41, 7.68, 7.74, 7.89, 7.89 (Ar-H), 9.15, 9.23 (-NH-).

Poly(DCPT-*p*PDA). FT-IR [KBr (cm^{-1})]: 3391 (N–H), 3272–3036 (aromatic C–H), 1550 (aromatic C=C), 1504 (triazine C=N), 1406, 801, 753, 694 (aromatic C–H), 1217 (aromatic C–N), 1406, 801, 753, 694 (aromatic C–H), 1218 (aromatic C–N). ^{1}H NMR (400 MHz, DMSO-d_6, ppm) δ 6.97, 7.15, 7.21, 7.31, 7.42 (Ar-H), 9.00, 9.04 (-NH-).

Poly(DCPT-*m*PDA). FT-IR [KBr (cm^{-1})]: 3377 (N–H), 3280–3110 (amine and guanamine hydrogen bonding), 3062 (aromatic C–H), 1615, 1575, 1547 (aromatic C=C), 1509 (triazine C=N), 1408, 804, 755, 693 (aromatic C–H), 1221 (aromatic C–N).

Poly(DCPT-BAFL). FT-IR [KBr (cm^{-1})]: 3395 (N–H), 3310–3080 (amine and guanamine hydrogen bonding), 3060 (aromatic C–H), 1592, 1544 (aromatic C=C), 1507 (triazine C=N), 1406, 806, 751, 694 (aromatic C–H), 1219 (aromatic C–N). ^{1}H NMR (400 MHz, DMSO-d_6, ppm) δ 6.72, 6.84, 7.08, 7.29, 7.35, 7.88 (Ar-H), 9.15 (-NH-).

Poly(BnDCT-*p*PDA). FT-IR [KBr (cm^{-1})]: 3398 (N–H), 3300–3080 (amine and guanamine hydrogen bonding), 3024, 2911 (aromatic and methylene group C–H), 1589, 1575 (aromatic C=C), 1511 (triazine C=N), 1404, 806, 726 (aromatic C–H), 1214 (aromatic C–N). ^{1}H NMR (400 MHz, DMSO-d_6, ppm) δ 4.51 (-CH2-), 7.19–7.65 (Ar-H), 8.92 (-NH-).

Poly(BnDCT-*m*PDA). FT-IR [KBr (cm^{-1})]: 3398 (guanamine hydrogen), 3026 (aromatic and methylene group C–H), 1583 (aromatic C=C), 1511 (triazine C=N), 1405, 806, 727 (aromatic C–H), 1189 (aromatic C–N). ^{1}H NMR (400 MHz, DMSO-d_6, ppm) δ 4.53 (-CH2-), 7.07–7.50 (Ar-H), 7.96 (-NH-CH2Ar), 8.82 (-NH-).

Poly(BnDCT-BAFL). FT-IR [KBr (cm^{-1})]: 3410 (N–H), 3380–3140 (amine and guanamine hydrogen bonding), 3060, 3028 (aromatic and methylene group C–H), 1575 (aromatic C=C), 1508 (triazine C=N), 1408, 809, 747 (aromatic C–H), 1222 (aromatic C–N). ^{1}H NMR (400 MHz, DMSO-d_6, ppm) δ 4.44 (-CH2-), 6.76–7.86 (Ar-H), 9.02 (-NH-).

Poly(αDCNmT-*p*PDA). FT-IR [KBr (cm^{-1})]: 3408 (N–H), 3280–3110 (amine and guanamine hydrogen bonding), 3039, 2911 (aromatic and methylene group C–H), 1575 (aromatic C=C), 1514 (triazine C=N), 1406, 806, 772, 726 (aromatic C–H), 1217 (aromatic C–N). ^{1}H NMR (400 MHz, DMSO-d_6, ppm) δ 4.98 (-CH2-), 7.46–8.15 (Ar-H), 8.93 (-NH-).

Poly(αDCNmT-*m*PDA). FT-IR [KBr (cm^{-1})]: 3400 (guanamine hydrogen), 3045 (aromatic and methylene group C–H), 1577 (aromatic C=C), 1508 (triazine C=N), 1414, 807, 772, 741 (aromatic C–H), 1193 (aromatic C–N). ^{1}H NMR (400 MHz, DMSO-d6, ppm) δ 4.98 (-CH2-), 7.46–7.95 (Ar-H), 8.15 (-NH-CH2), 8.93 (-NH-).

Poly(αDCNmT-BAFL). FT-IR [KBr (cm^{-1})]: 3413 (N–H), 3280–3100 (amine and guanamine hydrogen bonding), 3028 (aromatic and methylene group C–H), 1573 (aromatic C=C), 1509 (triazine C=N), 1409, 809, 748 (aromatic C–H), 1223 (aromatic C–N). ^{1}H NMR (400 MHz, DMSO-d_6, ppm) δ 4.93 (-CH2), 6.89–8.06 (Ar-H), 9.04 (-NH-).

Poly(βDCNT-*p*PDA). FT-IR [KBr (cm^{-1})]: 3402 (N–H), 3285–3060 (amine and guanamine hydrogen bonding), 3048 (aromatic C–H), 1561 (aromatic C=C), 1486 (triazine C=N), 1408, 804 (aromatic C–H), 1215 (aromatic C–N). ^{1}H NMR (400 MHz, DMSO- d_6, ppm) δ 7.30, 7.38, 7.79, 8.54 (Ar-H), 9.25, 9.44 (-NH-).

Poly(βDCNT-*m*PDA). FT-IR [KBr (cm^{-1})]: 3400 (N–H), 3298–3062 (amine and guanamine hydrogen bonding), 3048 (aromatic C–H), 1579 (aromatic C=C), 1484 (triazine C=N), 1409, 805 (aromatic C–H), 1192 (aromatic C–N). ^{1}H NMR (400 MHz, DMSO- d_6, ppm) δ 6.92–7.78, 8.03, 8.56 (Ar-H), 9.23, 9.45 (-NH-), 4.94 (terminal NH_2).

Poly(βDCNT-BAFL). FT-IR [KBr (cm^{-1})]: 3398 (N–H), 3052 (aromatic C–H), 1571 (aromatic C=C), 1484 (triazine C=N), 1412, 807, 746, (aromatic C–H), 1184 (aromatic C–N). ^{1}H NMR (400 MHz, DMSO-d_6, ppm) δ 7.05, 7.28, 7.34, 7.42, 7.72, 7.90, 8.46 (Ar-H), 9.30, 9.40 (-NH-).

Poly(βAntDCT-*p*PDA). FT-IR [KBr (cm^{-1})]: 3397 (N–H), 3036 (aromatic C–H), 1557 (aromatic C=C), 1514 (triazine C=N), 1406, 804, 740, (aromatic C–H), 1214 (aromatic C–N). ^{1}H NMR (400 MHz, DMSO-d_6, ppm) δ 7.32, 7.94, 8.38, 8.80 (Ar-H), 9.36, 9.56 (-NH-).

Poly(βAntDCT-*m*PDA). FT-IR [KBr (cm^{-1})]: 3399 (N–H), 3040 (aromatic C–H), 1578, 1556 (aromatic C=C), 1502 (triazine C=N), 1413, 804, 740, 688 (aromatic C–H), 1196 (aromatic C–N). ^{1}H NMR (400 MHz, DMSO-d_6, ppm) δ 7.33–8.53, 8.90 (Ar-H), 9.41, 9.65 (-NH-).

Poly(βAntDCT-BAFL). FT-IR [KBr (cm^{-1})]: 3398 (N–H), 3036 (aromatic C–H), 1572 (aromatic C=C), 1510, 1486 (triazine C=N), 1411, 806, 739 (aromatic C–H), 1182 (aromatic C–N). ^{1}H NMR (400 MHz, DMSO-d_6, ppm) δ 7.08, 7.30, 7.26, 7.54, 7.82, 8.03 (Ar-H), 9.44, 9.51 (-NH-).

Poly(αDCPyT-*p*PDA). FT-IR [KBr (cm^{-1})]: 3394 (N–H), 3036 (aromatic C–H), 1557 (aromatic C=C), 1514 (triazine C=N), 1404, 806, 710 (aromatic C–H), 1223 (aromatic C–N). ^{1}H NMR (400 MHz, DMSO-d_6, ppm) δ 7.53, 8.20, 8.82–8.99 (Ar-H), 9.37, 9.57 (-NH-).

Poly(αDCPyT-*m*PDA). FT-IR [KBr (cm^{-1})]: 3394 (N–H), 3036 (aromatic C–H), 1570 (aromatic C=C), 1509 (triazine C=N), 1411, 842, 748 (aromatic C–H), 1185 (aromatic C–N). ^{1}H NMR (400 MHz, DMSO-d_6, ppm) δ 6.78 (terminal NH_2), 8.05–8.36, 9.03 (Ar-H), 9.64, 9.73 (-NH-).

Poly(αDCPyT-BAFL). FT-IR [KBr (cm^{-1})]: 3394 (N–H), 3036 (aromatic C–H), 1570 (aromatic C=C), 1509 (triazine C=N), 1411, 842, 748 (aromatic C–H), 1185 (aromatic C–N). ^{1}H NMR (400 MHz, DMSO-d_6, ppm) δ 6.60–8.26 (Ar-H), 9.03–9.64 (-NH-).

Measurements. Fourier transform infrared (FT-IR) spectra were measured on a Jasco FT/IR-4200 spectrometer (Jasco Co. Ltd.) through transmittance absorption spectroscopy (KBr tablet method). The number-average molecular weights (M_n), weight-average molecular weights (M_w), and dispersities (M_w/M_n) of the PG samples were determined using a Tosoh HLC-8220 gel permeation chromatograph (GPC) equipped with refractive index and UV detectors and a consecutive polystyrene gel column (TSK-GEL α-M ×2) at 40 °C and eluted with NMP at a flow rate of 1.0 mL/min. Nuclear magnetic resonance (NMR) spectroscopy was performed on a Bruker AC-400P spectrometer at 400 MHz for ^{1}H and 100 MHz for ^{13}C measurements. Deuterated dimethyl sulfoxide (DMSO-d_6) was used as the solvent with tetramethylsilane as the internal reference. Thermal analyses were performed on a HITACHI TG/DTA7220 system at a heating rate of 10 °C/min for thermogravimetric analysis (TGA by TG/DTA 320) under air or

nitrogen. Differential scanning calorimetry was performed on a HITACHI X-DSC7000 system at a heating rate of 20 °C/min under nitrogen. UV-vis spectra were recorded on a SHIMAZU UV spectrophotometer (UV-1800). Fluorescence measurements were performed on a Jasco FP-6500 spectrometer with NMP. The excitation and emission band-paths were set at 3 nm. The scanning rate was 50 nm/min, and the measurements were repeated at least three times. The absolute fluorescence internal quantum yield (Φ_{fl}) of the sample solution in NMP (1.0×10^{-5} M) was determined with a JASCO FP-6500 fluorescence spectrophotometer attached to an ILF-533 100 mm ϕ integral sphere unit, with a band-path of 3 nm and scanning rate of 100 nm/min. The refractive indices were measured with a J.A. Woollam VASE ELLIPSOMETER. The 5 wt% polymer solution in NMP/cyclohexanone (9:1 v/v) was spin-coated at 200 rpm for 5 s and 1000 rpm for 30 s, followed by heating at 100 °C for 1 min and 250 °C for 5 min.

Conclusions

A series of rigid PG polymers bearing PAH pendants, such as naphthalene, anthracene, and pyrene, were successfully synthesized through conventional solution polymerization. All of the polymers showed high thermostabilities (T_g ~ 320, T_{d5} (N_2) ~ 466 °C, residue at 800 °C under nitrogen ~69.0%) and adequate solubilities in polar organic solvents. The films prepared by the solvent-cast method showed good transparencies with abnormally high refractive indices reaching 1.800 at the D-line (589 nm). The fluorescence spectra of the PG samples in solution revealed that when the PG chain contained bulky PAH and fluorenyl pendants, the chromophore could be isolated, resulting in a nearly quantitative quantum emission yield, even in polar organic solvents.

Acknowledgements

The authors express their sincerely gratitude to the Cooperative Research Program of "Network Joint Research Centre for Materials and Devices, 2015." The authors also would like to thank Iwate University Support Fund for Focused Research and for Formation of Centre of Excellence, 2013.

Notes and references

1 S. Ebihara, A. Okata, *Yuki Gosei Kagaku Kyokaishi* 1969, **27**, 1095.
2 M. Maciejewski, Z. Sektas, M. Bukowska, *Polimery* 1980, **25**, 358.
3 J.K. Lin, Y. Yuki, H. Kunisada, S. Kondo, *Polymer J.* 1990, **22**, 92.
4 H. Kunisada, Y. Yuki, S. Kondo, Y. Nishimori, A. Masuyama, *Polymer J.* 1991, **23**, 1455.
5 Y. Yuki, H. Kunisada, K. Iida, S. Kondo, *Polymer J.* 1995, **27**, 1239.
6 Y. Yuki, H. Kunisada, K. Iida, T. Kukaya, S. Kondo, *Polymer J.* 1996, **28**, 337.
7 Y. Yuki, H. Kunisada, K. Iida, S. Kondo, *Polymer J.* 1996, **28**, 553.
8 M. Maciejewski, E. Bednarek, J. Janiszewska, J. Janiszewski, G. Szczygiel, M. Zapora, *J. Macromol. Sci., Pure and Appl. Chem.* 2000, **A37**, 753.
9 Y. Oishi, T. Suzuki, H. Awano, K. Yonetaka, *IEEE Trans. Appl. Supercond.* 2004, **14**, 1604.
10 H. Koyano, K. Yoshihara, K. Ariga, T. Kunitake, Y. Oishi, O. Kawano, M. Kuramori, K. Suehiro, *J. Chem. Soc., Chem. Commun.* 1996, **15**, 1769.
11 H. Koyano, P. Bissel, K. Yoshihara, K. Ariga, T. Kunitake, *Langmuir* 1997, **13**, 5426.
12 J.K. Dixon, N.T. Woodberry, G.W. Costa, *J. Am. Chem. Soc.* 1947, **69**, 599.
13 S. Manna, A. Saha, A.K. Nandi, *Chem. Commun.* 2006, **41**, 4285.
14 A. Saha, S. Manna, A.K. Nandi, *Langmuir* 2007, **23**, 13126.
15 A. Saha, S. Manna, A.K. Nandi, *Chem. Commun.* 2008, **32**, 3732.
16 K.M. Anderson, G.M. Day, M.J. Paterson, P. Byrne, N. Clarke, J.W. Steed, *Angew. Chem. Int. Ed.* 2008, **47**, 1058.
17 Y. Shibasaki, T. Koizumi, N. Nishimura, Y. Oishi, *Chem. Lett.* 2011, **40**, 1132.
18 K. Saito, N. Nishimura, S. Sasaki, Y. Oishi, Y. Shibasaki, *React. & Function. Polym.* 2013, **73**, 756.
19 A. Fujimori, S. Miura, T. Kikkawa, Y. Shibasaki, *J. Polym. Sci., Part B: Polym. Phys.* 2015, **53**, 999.
20 G. Horowits, *Adv. Mater.* 1998, **10**, 365.
21 D. Adam, P. Schuhmacher, J. Simmerer, L. Häussling, K. Siemensmeyer, K.H. Etzbach, H. Ringsdorf, D. Haarer, D. *Nature*, 1994, **371**, 141.
22 L. Schmidt-Mende, A. Fechtenkötter, K. Müllen, E. Moons, R.H. Friend, J.D. MacKenzie, *Science*, 2001, **293**, 1119.

Synopsis